

# **UC Berkeley**

## **UC Berkeley Previously Published Works**

### **Title**

Laser-plasma ion beam booster based on hollow-channel magnetic vortex acceleration

### **Permalink**

<https://escholarship.org/uc/item/5bh0d8zz>

### **Journal**

Physical Review Research, 6(3)

### **Authors**

Garten, Marco

Bulanov, Stepan S

Hakimi, Sahel

et al.

### **Publication Date**

2024-08-07

### **DOI**

10.1103/physrevresearch.6.033148

### **Copyright Information**

This work is made available under the terms of a Creative Commons Attribution License, available at <https://creativecommons.org/licenses/by/4.0/>

Peer reviewed

## Laser-plasma ion beam booster based on hollow-channel magnetic vortex acceleration

Marco Garten<sup>1</sup>, Stepan S. Bulanov<sup>1</sup>, Sahel Hakimi<sup>1</sup>, Lieselotte Obst-Huebl<sup>1</sup>, Chad E. Mitchell<sup>1</sup>, Carl B. Schroeder<sup>1</sup>, Eric Esarey, Cameron G. R. Geddes<sup>1</sup>, Jean-Luc Vay<sup>1</sup>, and Axel Huebl<sup>1\*</sup>

*Accelerator Technology & Applied Physics Division, Lawrence Berkeley National Laboratory, 1 Cyclotron Road, Berkeley, California 94720, USA*



(Received 16 November 2023; accepted 12 June 2024; published 7 August 2024)

Laser-driven ion acceleration provides ultrashort, high-charge, low-emittance beams, which are desirable for a wide range of high-impact applications. Yet after decades of research, a significant increase in maximum ion energy is still needed. This paper introduces a quality-preserving staging concept for ultraintense ion bunches that is seamlessly applicable from the nonrelativistic plasma source to the relativistic regime. Full three-dimensional particle-in-cell simulations prove robustness and capture of a high-charge proton bunch, suitable for readily available and near-term laser facilities.

DOI: 10.1103/PhysRevResearch.6.033148

### I. INTRODUCTION

#### A. Laser-driven ion acceleration

Laser-driven ion acceleration provides unique particle bunches of very high charge ( $\gg 100$  pC), large current ( $>kA$ ), and ultralow emittance ( $\ll 10$  nm) on very compact acceleration footprints [1–6]. Such high-intensity ion beams can have a significant impact on advancing both fundamental and applied research applications in physics, industry, and society, ranging from next-generation hadron colliders or neutrino factories [7,8], drivers for inertial fusion energy [9,10], radiotherapy [11–16], nuclear physics [17], warm-dense matter research [18,19], secondary radiation generation [20,21] for material research and security applications, and possibly even radiation hardness of spacecraft [22,23]. However, after decades of research, the demonstrated maximum particle energy, between 60 and 150 MeV for protons [24–28], still remains short of desired ranges for many of the mentioned pivotal applications.

With state-of-the-art petawatt (PW) laser facilities [29,30] that can deliver high-intensity laser pulses reaching  $10^{23}$  W/cm<sup>2</sup> [31], laser-ion acceleration remains an indirect process due to the high mass of ions. The laser pulse interacts primarily with plasma electrons, creating a localized ( $<\mu\text{m}$ ) charge separation that imposes a strong ( $>\text{TV/m}$ ) electric field, orders of magnitude higher than achievable in established cyclotrons and radio-frequency accelerators, which then facilitates the acceleration. Depending on the laser intensity and contrast [2,25,32], target density, thickness, and composition, a specific laser-ion acceleration mechanism might dominate [1–3,33]. In these mechanisms, the maximum ion energy scales with laser intensity on target, for some

even linearly, while demanding high control of temporal laser contrast [33]. Yet, increasing laser power is a multidecade-long undertaking, and significant advances initially reduce laser repetition rate and temporal laser contrast, and increase facility cost and footprint [29,30].

In this paper, we propose a solution to the longstanding challenge of achieving relativistic ion energies from a laser-plasma accelerator, the first quality-preserving, self-consistently modeled concept of ion staging. This concept for staging boosts particle energies from the subrelativistic over arbitrary energy levels to the relativistic regime. Staging was already demonstrated in the plasma acceleration of electrons [34,35] and is a candidate for next-generation electron-positron colliders for high-energy physics and light sources [36]. In contrast to staged electron acceleration, where the initial laser-plasma source readily provides relativistic particles, ions need to be accelerated in multiple stages while undergoing significant velocity changes. In this paper, we present an ultracompact stage with quasistatic fields of a specifically designed laser-driven plasma element [see Fig. 1 for a three-dimensional (3D) visualization] and show that repeated injection into stages of the same compact design boosts ion energy progressively from nonrelativistic to relativistic values.

#### B. Magnetic vortex acceleration

This paper explores staging via a laser-target setup previously used for magnetic vortex acceleration (MVA) [37–39]. Realizing MVA involves the interaction of an intense laser pulse with a near-critical density (NCD),  $n_e \approx n_{cr}$ , plasma target of several tens of micrometer thickness [40–42]. Here,  $n_e$  and  $n_{cr} = m_e \omega^2 / 4\pi e^2$  are the plasma density and critical plasma density,  $e$  and  $m_e$  are electron charge and mass, and  $\omega$  is the central laser pulse frequency. The ponderomotive force of the laser pulse generates a plasma channel, first in electron density, then in ion density. During its propagation through the channel, the laser pulse causes a strong electron current in the forward direction, which later starts to pinch, creating an electron and ion filament along the laser propagation axis. As the laser, electrons, and ions exit the target from the back side,

\*Contact author: axelhuebl@lbl.gov

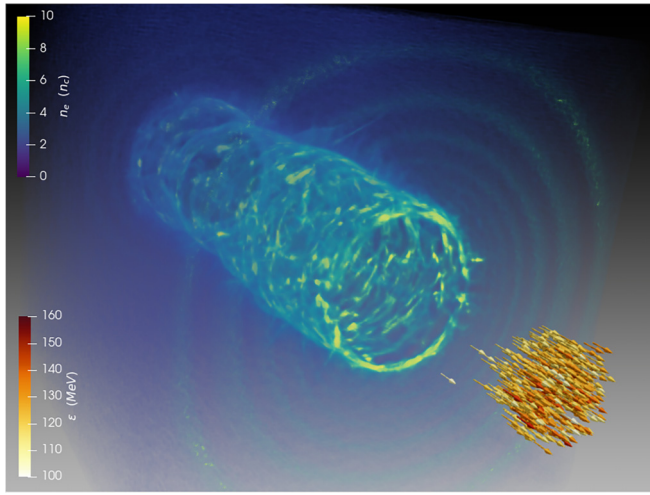


FIG. 1. Volumetric rendering of the electron density  $n_e$  at the exit of the plasma booster stage with selected bunch protons colored by kinetic energy (arrows).

strong electric ( $\sim$ TV/m) and magnetic fields ( $\sim 10^4$  T) are generated there, arising from the forward-accelerated electron filament and cold return currents in the channel walls. This produces a high-flux ion beam of ultrashort time structure and with nanocoulombs of charge [37,38].

For MVA, the electric fields created at the rear side of the plasma channel both accelerate and focus the ions. Ion acceleration from near-critical density plasmas has been studied in multiple experiments [27,43–48], and MVA was found to be robust against laser contrast and incidence angle variations in numerical modeling studies [39]. The near-critical density regime of MVA, readily reached with high-repetition rate targets [27,49], relaxes the requirements for microscopic fabrication precision needed. Particularly attractive for energy boosting is that upon laser irradiation no potential barrier is created at the target front side, which would decelerate particles [50–53].

### C. Related work

Existing theoretical work on boosting the energy of laser-driven ion beams can be classified into different categories: first, energy boosting from a cascade of acceleration mechanisms, using a single laser pulse and composite target [54–57] or multiple targets [58,59], and second, energy boosting using multiple laser pulses on a single target [60–63]. The first approach is limited by the available laser energy, and the second is sensitive to control of the spatiotemporal laser-plasma interaction. The third category is proposing to avoid these limitations, energy boosting with multiple laser pulses and staged targets [50,52,64,65], so far with limited exploration of performance with intense beams or preservation of important beam moments, besides gaining energy. Consequently, no experimental studies exist so far.

## II. METHODS

### A. Booster stage design

Here, MVA is studied as a scalable mechanism for boosting an ultraintense, high-charge beam that is implementable

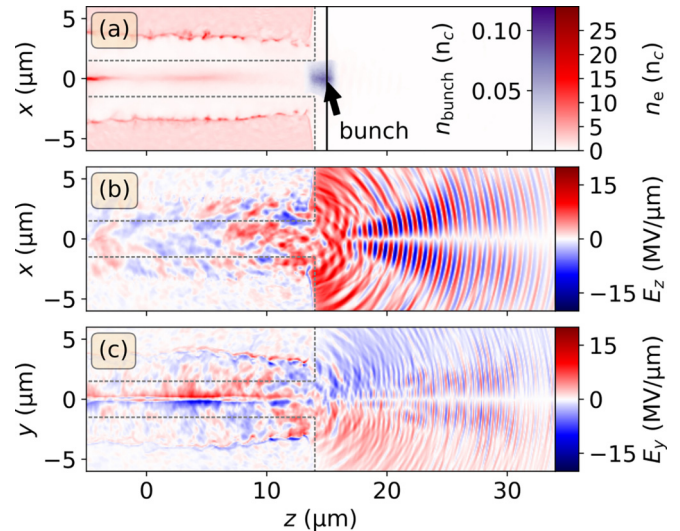


FIG. 2. Fields of the booster stage, loaded with a 200 pC proton bunch. The stage center is at  $z = 0 \mu\text{m}$ . (a) Electron density  $n_e$  in red, reference plane at the accelerating bucket  $z_{ab} = 15 \mu\text{m}$  (black vertical line), and beam density  $n_{\text{bunch}}$  in purple located behind the exit of the stage. (b) Accelerating electric field  $E_z$ , and (c) focusing electric field  $E_y$ , all shown as the beam reaches  $z_{ab}$ . Dashed gray lines mark the outline of the initial electron density of the hollow channel.

with high-repetition rate stages [27,49,66]. We investigate and propose a robust, quality-preserving variation of MVA as a plasma booster, which is insensitive to the accepted ion beam velocities, and systematically evaluate temporal and spatial acceptance tolerances. Critical for staging into subsequent high- $\beta$  (normalized ion velocity  $\beta = v/c$ ) acceleration stages, our approach can conserve the high charge and the ultralow emittance of laser-plasma generated beams. The presented booster also accepts substantial energy spreads.

However, there is a significant distinction between a typical MVA target and the one proposed here, visualized in Fig. 2. In MVA, the accelerated ions originate from a central filament, which is formed from the background ions under the action of the pinched electron current. Those ions mainly come from a small region at the back of the target near the channel axis. Thus, in order to suppress additional low-energy ion injection from the booster stage itself, an NCD target with a preformed hollow region is chosen (dashed lines in Fig. 2) [67–70].

Typically, MVA relies on the intense laser pulse self-channeling in an NCD plasma [37,38,71]. The balance of the ponderomotive push by the laser and the Coulomb attraction between the displaced electrons and remaining ions determine the radius of such a channel. In the case of an NCD plasma with a preformed channel of radius  $r_h$  [for simplicity we simulate a density step function  $n_e(r < r_h) = 0$ ], the radius of the self-generated channel  $R_{\text{ch}}$  and the amplitude of the laser field  $a_{\text{ch}}$  in the channel can be determined using the same line of reasoning:

$$\frac{\pi^2}{\lambda^2} (R_{\text{ch}}^2 - r_h^2) = a_{\text{ch}}(r_h) \frac{n_{\text{cr}}}{n_e}, \quad (1)$$

$$\frac{\pi^2 R_{\text{ch}}^2}{\lambda^2} a_{\text{ch}}^2 = \frac{2P}{K P_c}. \quad (2)$$

Here,  $a_{\text{ch}}(r_h) = a_{\text{ch}}[J_0(\kappa r_h) - J_2(\kappa r_h)]$ , which comes from the solution of the wave equation in the waveguide [37],  $J_0$  and  $J_2$  are the Bessel functions, and  $\kappa = 1.84/R_{\text{ch}}$ .  $P_c = 8\pi\epsilon_0 m_e^2 c^5/e^2 = 17 \text{ GW}$  is a characteristic power for relativistic self-focusing,  $\lambda$  and  $P$  are the laser wavelength and power, respectively, and  $K = 1/13.5$  is a geometric factor. In the case  $r_h = 0$ , these two equations reduce to the results of Ref. [71]. For the parameters used below, the radius of the channel is  $R_{\text{ch}} = 2.1 \mu\text{m}$ , which is only 5% smaller than in the case of a homogeneous NCD plasma.

As mentioned above, the accelerating and focusing fields at the back of the target are due to the strong electron current flowing through the channel, following the laser pulse. The peak value of the magnetic field generated by such a current scales as  $B_{\text{ch}} \sim n_e R_{\text{ch}}^3$ . Thus, the main difference in field strength between homogeneous and hollow targets is caused by a factor  $(1 - r_h^2/R_{\text{ch}}^2)$  difference of electrons available in the channel.

## B. Simulation setup

For the study of the booster concept, three-dimensional electromagnetic particle-in-cell simulations with the code WarpX [72,73] are performed, using parameters readily available at existing PW laser facilities such as the BELLA iP2 beamline [74]. The laser pulse in all simulations discussed in this paper has 9.6 J of energy on target (Gaussian, central laser mode), a normalized amplitude of  $a_0 = 42$ , a central wavelength of 815 nm, a duration of 29.8 fs, a beam waist of  $2.12 \mu\text{m}$ , and is linearly polarized (in  $x$ ).

The booster stage targets are each  $28 \mu\text{m}$  in length, with a density of  $2n_{\text{cr}}$  and preformed channel radius of  $r_h = 1.5 \mu\text{m}$ . The hollow channel prevents interactions between the ion beam and the plasma within  $r_h$ , which would otherwise impact the beam quality. The laser pulse waist is larger than the preformed channel, so as to drive a strong channel current at radius  $R_{\text{ch}}$  for acceleration at the stage rear. The laser-target interaction pulls electrons off the channel wall and creates a forward-propagating electron filament on the channel axis, as in regular MVA (see Fig. 2). When the laser pulse and the electron filament pass the target rear, MVA-type accelerating and focusing fields are created, forming an “accelerating bucket.” The ion beam experiences optimal acceleration before the electron filament disperses and field strengths subside. It is temporally phase matched to the peak field in space  $z_{\text{ab}}$  and time.

## III. RESULTS

### A. Single-particle acceptance

Before exploring the collective boost of a high-charge bunch, the properties of the hollow MVA stage in terms of longitudinal and transverse single-particle acceptance are studied. Characterizing the proton phase space that can be energy boosted, noninteracting protons are varied in initial position and momentum space and tracked through the electromagnetic fields of the self-consistently modeled laser-driven plasma stage.

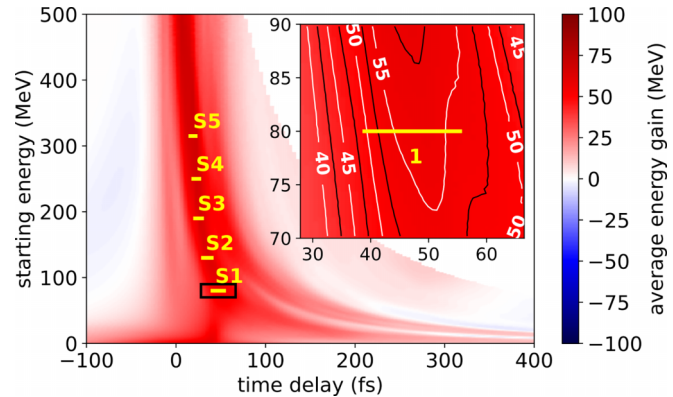


FIG. 3. Longitudinal beam acceptance. Average energy gain for tracked beam particles vs their starting energy and arrival time offset with respect to the laser maximum at  $z_{\text{ab}} = 15 \mu\text{m}$ . The laser maximum is behind (before) the particle beam for negative (positive) times. Yellow horizontal lines mark design energies for five consecutive stages (S1–S5) to boost a beam from 80 to 380 MeV starting energy. The inset shows a zoomed detail for stage 1, with a “flattened” region of uniform acceleration for intense beams of up to 15 fs in duration.

### 1. Longitudinal acceptance

Figure 3 shows the longitudinal bunch acceptance, a measure for accepted bunch length and temporal jitter between bunch particles and laser pulse with respect to a reference plane at  $z_{\text{ab}}$ . Since the incoming ion beam is nonrelativistic for early stages, it is timed to enter the plasma stage before the laser pulse and is overtaken by it during the course of the propagation. Tracked particles were initially uniformly distributed within  $0 \leq r_0 \leq 0.25 \mu\text{m}$  and without transverse momentum.

As long as the particle bunch arrives with or after the laser maximum in the accelerating bucket, for a large tolerance of over 200 fs, an energy boost between 30 and 80 MeV is observed. Particles that arrive outside this window are decelerated by less than 15 MeV. In Fig. 3, five possible consecutive stages are marked from 80 to 380 MeV. The inset shows a zoomed detail for stage 1, with a “flattened” region of uniform acceleration for intense beams of up to 15 fs in duration.

### 2. Transverse acceptance

Figure 4 shows the correlation of transverse normalized momenta with radial position for beam acceptance into the booster stage. For each stage S1–S5 in Fig. 3, protons were tracked for a range of transverse initial conditions, and initial longitudinal momenta corresponding to their marked energies, respectively.

Every bunch initially measured  $2 \mu\text{m}$  in length and  $4 \mu\text{m}$  in diameter, was uniformly distributed and centered around a  $z$  position corresponding to the delay expected to deliver the highest-energy boost. Transverse momenta were also uniformly distributed. A fraction of particles traversed the background plasma in the channel wall region to check that the transverse acceptance is not limited by the channel aperture, e.g., due to laser-plasma interaction dynamics. Accommodating the cylindrical channel symmetry, we show the normalized radial momentum  $p_r/p_z$  versus radial distance  $r$ , where  $p_r = (p_x^2 + p_y^2)^{1/2}$ . For Fig. 4, particles had initial

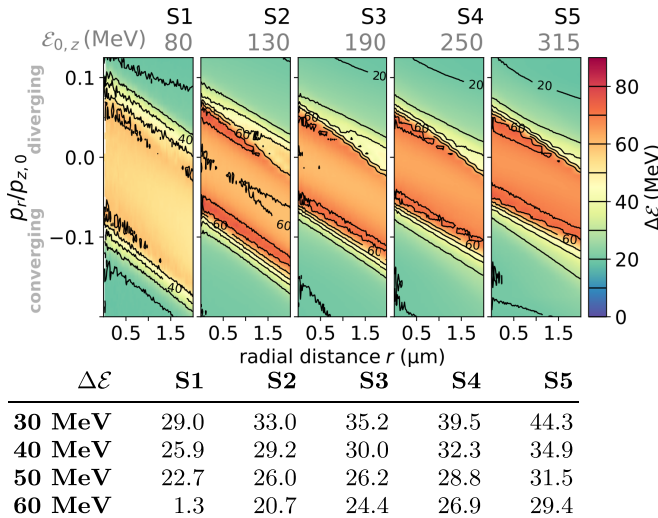


FIG. 4. Transverse beam acceptance. Top: Average energy gain  $\Delta\epsilon$  of tracked particles with respect to initial radial distance  $r$  and initial normalized transverse momentum  $p_r/p_{z,0}$ . Bottom: Maximum accepted normalized transverse emittance in nm. Values are for minimum energy gains  $\Delta\epsilon$  of 30, 40, 50, and 60 MeV per stage, respectively.

azimuthal momenta  $p_\theta/mc$  smaller than 0.02. As before, the total energy gain is color coded. Spaced at every 10 MeV, contour lines mark a constant energy gain between 0 and 90 MeV. Slightly diverging particles on axis are still accepted by the stage. With growing radial distance only focused, converging particles (negative normalized radial momentum) are still accepted. Interestingly, for beams with initial energies larger than 130 MeV, particles with a specific position-angle relation not aligned with the central propagation axis gain the highest energies in the stages S2–S5.

Calculated from the phase-space regions contained in the respective contours in Fig. 4, the table lists the maximum accepted transverse emittances for each stage and selected minimum energy boosts: For a beam with a Kapchinskij-Vladimirskij (KV) distribution [75], one can estimate this maximum accepted emittance by dividing the phase-space area by  $2\pi$  (instead of  $4\pi$ , due to the projection of phase space to radial distance instead of the transverse position) and multiplying by  $p_{0,z}/mc$ . For boosts between 30 and 50 MeV, all stages accept a bunch with normalized emittance up to 23–44 nm. The accepted emittance is sufficient for bunches of MVA sources (<20 nm) and even increases acceptance for higher input energies.

## B. Self-consistent, high-charge acceleration

Including all collective effects of the energy-boosted beam, Figs. 1, 2, and 5 present a fully self-consistent electromagnetic 3D WarpX simulation with an ultraintense (19.3 kA), high-charge (200 pC), narrowly focused proton bunch. Informed by Figs. 3 and 4, bunch parameters are a transverse KV distribution, uniform in time, and a Gaussian, sub-relativistic of  $80 \pm 5$  MeV (energy spread  $\sigma_\epsilon = 5.1\%$ ). In practice, the 200 pC of charge could be energy selected from a wider spectrum of a present day PW laser ion source and ideally

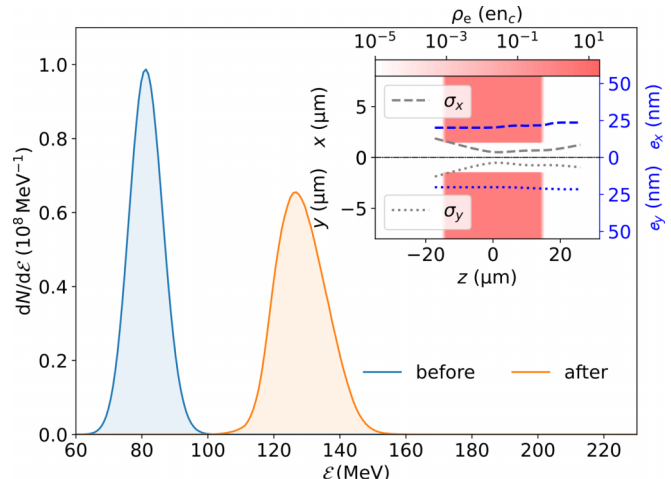


FIG. 5. Energy spectrum of a 200 pC proton beam before (blue) and after (orange) the MVA booster element. The inset shows the initial electron density distribution (red shaded area) of the stage in the  $x-z$  and  $y-z$  half planes. Furthermore, gray lines show the evolution of transverse root mean square beam sizes  $\sigma_x$  (dashed) and  $\sigma_y$  (dotted, mirrored downwards) along the longitudinal coordinate. Blue lines show the evolution of normalized transverse emittance  $e_x$  (dashed) and  $e_y$  (dotted), respectively.

transported via an apochromatic beamline [76–78]. It is assumed that the bunch has been phase-space rotated in a similar fashion as described by Busold *et al.* [79].

The inset of Fig. 5 presents the bunch envelope and emittance evolution. Performed beam-loaded 3D simulations showed that emittance growth from a space charge and subsequent channel-wall interaction occur in the second half of the channel ( $z > 0$ ). Mitigating this effect, the proton beam focal position was adjusted from  $z_{ab}$  at the target rear to  $z_f = 3 \mu\text{m}$ , exploiting that the beam is pinched in the strong laser-induced fields of the plasma channel (gray lines).

Fixing the transverse bunch size in focus ( $2\sigma_{x,y} = 1 \mu\text{m}$ ) and choosing the transverse emittance to be between results from Hakimi *et al.* [39] and the maximum accepted emittance from Fig. 4, namely  $e_x = e_y = 20 \text{ nm}$ , results in the Courant-Snyder (Twiss) parameters at the initialization plane at  $\langle z \rangle_0 = -17.3 \mu\text{m}$ :  $\beta_{x,0} = \beta_{y,0} = 74.2 \mu\text{m}$ ,  $\alpha_{x,0} = \alpha_{y,0} = 3.62$ , and  $\gamma_{x,f} = \gamma_{y,f} = 190\,000 \text{ m}^{-1}$  via the beam envelope equations [80] for a drift.

The central bunch energy is boosted in the stage by 50 MeV, as predicted by tracking simulations in Fig. 3. No bunch charge is lost during the acceleration process. The energy spread grew from 5% to 7%. After the first booster stage, the emittance has grown by only 3.5 nm. These results are well within range for the above predicted coupling requirements to higher-energy stages and provide the opportunity for future research on design optimizations for energy boosting to multiple stages.

## IV. SUMMARY AND CONCLUSIONS

In summary, a self-consistently modeled scheme is presented for boosting the energy of ultra-intense ion bunches of arbitrary  $\beta$ : Staging can overcome the limits of achiev-

able beam energy in a single laser-plasma interaction, which currently impedes the impact of laser-driven ion acceleration. Central for a staging approach, 3D simulations confirm the conservation of charge, energy spread, and emittance. Additionally, the same laser-plasma stage can be used for a scalable range of input velocities, facilitating the coupling of multiple stages via the control of the temporal delay between laser pulse and boosted ion bunch. Benefiting from the combined strong acceleration and focusing fields in magnetic vortex acceleration (tens of MV/ $\mu$ m), a hollow target is suitable as a robust plasma booster stage. Source and booster laser-plasma parameter ranges are realistic for state-of-the-art and upcoming laser facilities around the world [74,81], motivating experimental validation and implementation for applications.

### ACKNOWLEDGMENTS

We thank R. T. Sandberg, D. Terzani, R. Lehe, and J. Qiang for helpful discussions. Simulations used the open source particle-in-cell code WarpX in version 23.01. Primary WarpX

contributors are with LBNL, LLNL, CEA-LIDYL, SLAC, DESY, CERN, and TAE Technologies. We acknowledge all WarpX contributors. Simulation inputs, analysis scripts, source code, and data are available in Refs. [73,82]. This material is based upon work supported by the Defense Advanced Research Projects Agency (DARPA) via Northrop-Grumman Corporation. Partly supported by the U.S. DOE FES Postdoctoral Research Program via ORISE under Contract No. DE-SC0014664, the U.S. DOE Office of Science Offices of ASCR, HEP, and FES (including LaserNetUS) under Contract No. DE-AC02-05CH11231, and the Exascale Computing Project (17-SC-20-SC). This research used resources of the Oak Ridge Leadership Computing Facility at the Oak Ridge National Laboratory, which is supported by the Office of Science of the U.S. Department of Energy under Contract No. (DE-AC05-00OR22725, as part of an ASCR Leadership Computing Challenge (ALCC) award and the National Energy Research Scientific Computing Center (NERSC), a Department of Energy Office of Science User Facility using NERSC award FES-ERCAP0024250).

- 
- [1] G. A. Mourou, T. Tajima, and S. V. Bulanov, Optics in the relativistic regime, *Rev. Mod. Phys.* **78**, 309 (2006).
  - [2] H. Daido, M. Nishiuchi, and A. S. Pirozhkov, Review of laser-driven ion sources and their applications, *Rep. Prog. Phys.* **75**, 056401 (2012).
  - [3] A. Macchi, M. Borghesi, and M. Passoni, Ion acceleration by superintense laser-plasma interaction, *Rev. Mod. Phys.* **85**, 751 (2013).
  - [4] T. E. Cowan, J. Fuchs, H. Ruhl, A. Kemp, P. Audebert, M. Roth, R. Stephens, I. Barton, A. Blazevic, E. Brambrink, J. Cobble, J. Fernández, J.-C. Gauthier, M. Geissel, M. Hegelich, J. Kaae, S. Karsch, G. P. Le Sage, S. Letzring, M. Mancossi *et al.*, Ultralow emittance, multi-MeV proton beams from a laser virtual-cathode plasma accelerator, *Phys. Rev. Lett.* **92**, 204801 (2004).
  - [5] M. Borghesi, A. J. Mackinnon, D. H. Campbell, D. G. Hicks, S. Kar, P. K. Patel, D. Price, L. Romagnani, A. Schiavi, and O. Willi, Multi-MeV proton source investigations in ultraintense laser-foil interactions, *Phys. Rev. Lett.* **92**, 055003 (2004).
  - [6] F. Nürnberg, M. Schollmeier, E. Brambrink, A. Blažević, D. C. Carroll, K. Flippo, D. C. Gautier, M. Geißel, K. Harres, B. M. Hegelich, O. Lundh, K. Markey, P. McKenna, D. Neely, J. Schreiber, and M. Roth, Radiochromic film imaging spectroscopy of laser-accelerated proton beams, *Rev. Sci. Instrum.* **80**, 033301 (2009).
  - [7] A. Abada, M. Abbrescia, S. S. AbdusSalam, I. Abdyukhanov, J. Abelleira Fernandez, A. Abramov, M. Aburaia, A. O. Acar, P. R. Adzic, P. Agrawal *et al.* (The FCC Collaboration), FCC-hh: The hadron collider, *Eur. Phys. J.: Spec. Top.* **228**, 755 (2019).
  - [8] S. Geer and M. S. Zisman, Neutrino factories: Realization and physics potential, *Prog. Part. Nucl. Phys.* **59**, 631 (2007).
  - [9] M. Roth, T. E. Cowan, M. H. Key, S. P. Hatchett, C. Brown, W. Fountain, J. Johnson, D. M. Pennington, R. A. Snavely, S. C. Wilks, K. Yasuike, H. Ruhl, F. Pegoraro, S. V. Bulanov, E. M. Campbell, M. D. Perry, and H. Powell, Fast ignition by intense laser-accelerated proton beams, *Phys. Rev. Lett.* **86**, 436 (2001).
  - [10] A. J. Mackinnon, P. K. Patel, M. Borghesi, R. C. Clarke, R. R. Freeman, H. Habara, S. P. Hatchett, D. Hey, D. G. Hicks, S. Kar, M. H. Key, J. A. King, K. Lancaster, D. Neely, A. Nikkro, P. A. Norreys, M. M. Notley, T. W. Phillips, L. Romagnani, R. A. Snavely *et al.*, Proton radiography of a laser-driven implosion, *Phys. Rev. Lett.* **97**, 045001 (2006).
  - [11] V. Favaudon, L. Caplier, V. Monceau, F. Pouzoulet, M. Sayarath, C. Fouillade, M.-F. Poupon, I. Brito, P. Hupé, J. Bourhis, J. Hall, J.-J. Fontaine, and M.-C. Vozenin, Ultrahigh dose-rate FLASH irradiation increases the differential response between normal and tumor tissue in mice, *Sci. Transl. Med.* **6**, 245ra93 (2014).
  - [12] P. Montay-Gruel, K. Petersson, M. Jaccard, G. Boivin, J.-F. Germond, B. Petit, R. Doenlen, V. Favaudon, F. Bochud, C. Bailat, J. Bourhis, and M.-C. Vozenin, Irradiation in a flash: Unique sparing of memory in mice after whole brain irradiation with dose rates above 100Gy/s, *Radiotherapy Oncol.* **124**, 365 (2017).
  - [13] J. Bin, L. Obst-Huebl, J.-H. Mao, K. Nakamura, L. D. Geulig, H. Chang, Q. Ji, L. He, J. De Chant, Z. Kober, A. J. Gonsalves, S. Bulanov, S. E. Celiker, C. B. Schroeder, C. G. R. Geddes, E. Esarey, B. A. Simmons, T. Schenkel, E. A. Blakely, S. Steinke *et al.*, A new platform for ultra-high dose rate radiobiological research using the BELLA PW laser proton beamline, *Sci. Rep.* **12**, 1484 (2022).
  - [14] S. V. Bulanov and V. S. Khoroshkov, Feasibility of using laser ion accelerators in proton therapy, *Plasma Phys. Rep.* **28**, 453 (2002).
  - [15] S. V. Bulanov, J. J. Wilkens, T. Z. Esirkepov, G. Korn, G. Kraft, S. D. Kraft, M. Molls, and V. S. Khoroshkov, Laser ion acceleration for hadron therapy, *Phys. Usp.* **57**, 1149 (2014).
  - [16] L. Karsch, E. Beyreuther, W. Enghardt, M. Gotz, U. Masood, U. Schramm, K. Zeil, and J. Pawelke, Towards ion beam therapy based on laser plasma accelerators, *Acta Oncol.* **56**, 1359 (2017).
  - [17] S. N. Chen, F. Negoita, K. Spohr, E. d'Humières, I. Pomerantz, and J. Fuchs, Extreme brightness laser-based neutron pulses as

- a pathway for investigating nucleosynthesis in the laboratory, *Matter Radiat. Extremes* **4**, 054402 (2019).
- [18] M. Borghesi, A. Schiavi, D. H. Campbell, M. G. Haines, O. Willi, A. J. MacKinnon, L. A. Gizzi, M. Galimberti, R. J. Clarke, and H. Ruhl, Proton imaging: A diagnostic for inertial confinement fusion/fast ignitor studies, *Plasma Phys. Controlled Fusion* **43**, A267 (2001).
- [19] A. Pelka, G. Gregori, D. O. Gericke, J. Vorberger, S. H. Glenzer, M. M. Günther, K. Harres, R. Heathcote, A. L. Kritch, N. L. Kugland, B. Li, M. Makita, J. Mithen, D. Neely, C. Niemann, A. Otten, D. Riley, G. Schaumann, M. Schollmeier, A. Tauschwitz, and M. Roth, Ultrafast melting of carbon induced by intense proton beams, *Phys. Rev. Lett.* **105**, 265701 (2010).
- [20] K. W. D. Ledingham, P. McKenna, and R. P. Singhal, Applications for nuclear phenomena generated by ultra-intense lasers, *Science* **300**, 1107 (2003).
- [21] V. I. Yurevich, Production of neutrons in thick targets by high-energy protons and nuclei, *Phys. Part. Nuclei* **41**, 778 (2010).
- [22] M. Durante and F. A. Cucinotta, Physical basis of radiation protection in space travel, *Rev. Mod. Phys.* **83**, 1245 (2011).
- [23] Y. Miyazawa, M. Ikegami, H.-W. Chen, T. Ohshima, M. Imaizumi, K. Hirose, and T. Miyasaka, Tolerance of perovskite solar cell to high-energy particle irradiations in space environment, *iScience* **2**, 148 (2018).
- [24] F. Wagner, O. Deppert, C. Brabec, P. Fiala, A. Kleinschmidt, P. Poth, V. A. Schanz, A. Tebartz, B. Zielbauer, M. Roth, T. Stöhlker, and V. Bagnoud, Maximum proton energy above 85 MeV from the relativistic interaction of laser pulses with micrometer thick CH<sub>2</sub> targets, *Phys. Rev. Lett.* **116**, 205002 (2016).
- [25] A. Higginson, R. J. Gray, M. King, R. J. Dance, S. D. R. Williamson, N. M. H. Butler, R. Wilson, R. Capdessus, C. Armstrong, J. S. Green, S. J. Hawkes, P. Martin, W. Q. Wei, S. R. Mirfayzi, X. H. Yuan, S. Kar, M. Borghesi, R. J. Clarke, D. Neely, and P. McKenna, Near-100 MeV protons via a laser-driven transparency-enhanced hybrid acceleration scheme, *Nat. Commun.* **9**, 724 (2018).
- [26] N. P. Dover, T. Ziegler, S. Assenbaum, C. Bernert, S. Bock, F.-E. Brack, T. E. Cowan, E. J. Ditter, M. Garten, L. Gaus, I. Goethel, G. S. Hicks, H. Kiriyama, T. Kluge, J. K. Koga, A. Kon, K. Kondo, S. Kraft, F. Kroll, H. F. Lowe *et al.*, Enhanced ion acceleration from transparency-driven foils demonstrated at two ultraintense laser facilities, *Light: Sci. Appl.* **12**, 71 (2023).
- [27] M. Rehwald, S. Assenbaum, C. Bernert, F.-E. Brack, M. Bussmann, T. E. Cowan, C. B. Curry, F. Fiuza, M. Garten, L. Gaus, M. Gauthier, S. Göde, I. Göthel, S. H. Glenzer, L. Huang, A. Huebl, J. B. Kim, T. Kluge, S. Kraft, F. Kroll *et al.*, Ultra-short pulse laser acceleration of protons to 80 MeV from cryogenic hydrogen jets tailored to near-critical density, *Nat. Commun.* **14**, 4009 (2023).
- [28] T. Ziegler, I. Göthel, S. Assenbaum, C. Bernert, F.-E. Brack, T. E. Cowan, N. P. Dover, L. Gaus, T. Kluge, S. Kraft, F. Kroll, J. Metzkes-Ng, M. Nishiuchi, I. Prencipe, T. Püschel, M. Rehwald, M. Reimold, H.-P. Schlenvoigt, M. E. P. Umlandt, M. Vescovi *et al.*, Laser-driven high-energy proton beams from cascaded acceleration regimes, *Nat. Phys.* **20**, 1211 (2024).
- [29] C. N. Danson, C. Haefner, J. Bromage, T. Butcher, J.-C. F. Chanteloup, E. A. Chowdhury, A. Galvanauskas, L. A. Gizzi, J. Hein, D. I. Hillier *et al.*, Petawatt and exawatt class lasers worldwide, *High Power Laser Sci. Eng.* **7**, e54 (2019).
- [30] A. Gonoskov, T. G. Blackburn, M. Marklund, and S. S. Bulanov, Charged particle motion and radiation in strong electromagnetic fields, *Rev. Mod. Phys.* **94**, 045001 (2022).
- [31] J. W. Yoon, Y. G. Kim, I. Choi, J. H. Sung, H. W. Lee, S. K. Lee, and C. H. Nam, Realization of laser intensity over 10<sup>23</sup> W/cm<sup>2</sup>, *Optica* **8**, 630 (2021).
- [32] T. Ziegler, D. Albach, C. Bernert, S. Bock, F. E. Brack, T. E. Cowan, N. P. Dover, M. Garten, L. Gaus, R. Gebhardt, I. Goethel, U. Helbig, A. Irman, H. Kiriyama, T. Kluge, A. Kon, S. Kraft, F. Kroll, M. Loeser, J. Metzkes-Ng *et al.*, Proton beam quality enhancement by spectral phase control of a PW-class laser system, *Sci. Rep.* **11**, 7338 (2021).
- [33] S. S. Bulanov, E. Esarey, C. B. Schroeder, S. V. Bulanov, T. Z. Esirkepov, M. Kando, F. Pegoraro, and W. P. Leemans, Radiation pressure acceleration: The factors limiting maximum attainable ion energy, *Phys. Plasmas* **23**, 056703 (2016).
- [34] S. Steinke, J. van Tilborg, C. Benedetti, C. G. R. Geddes, C. B. Schroeder, J. Daniels, K. K. Swanson, A. J. Gonsalves, K. Nakamura, N. H. Matlis, B. H. Shaw, E. Esarey, and W. P. Leemans, Multistage coupling of independent laser-plasma accelerators, *Nature (London)* **530**, 190 (2016).
- [35] T. Kurz, T. Heinemann, M. F. Gilljohann, Y. Y. Chang, J. P. Couperus Cabadağ, A. Debus, O. Kononenko, R. Pausch, S. Schöbel, R. W. Assmann, M. Bussmann, H. Ding, J. Götzfried, A. Köhler, G. Raj, S. Schindler, K. Steiniger, O. Zarini, S. Corde, A. Döpp *et al.*, Demonstration of a compact plasma accelerator powered by laser-accelerated electron beams, *Nat. Commun.* **12**, 2895 (2021).
- [36] C. Geddes, M. Hogan, P. Musumeci, and R. Assmann, Report of snowmass 21 accelerator frontier topical group 6 on advanced accelerators, *arXiv:2208.13279*.
- [37] S. S. Bulanov, V. Y. Bychenkov, V. Chvykov, G. Kalinchenko, D. W. Litzenberg, T. Matsuoka, A. G. R. Thomas, L. Willingale, V. Yanovsky, K. Krushelnick, and A. Maksimchuk, Generation of GeV protons from 1 PW laser interaction with near-critical density targets, *Phys. Plasmas* **17**, 043105 (2010).
- [38] J. Park, S. S. Bulanov, J. Bin, Q. Ji, S. Steinke, J.-L. Vay, C. G. R. Geddes, C. B. Schroeder, W. P. Leemans, T. Schenkel, and E. Esarey, Ion acceleration in laser-generated megatesla magnetic vortex, *Phys. Plasmas* **26**, 103108 (2019).
- [39] S. Hakimi, L. Obst-Huebl, A. Huebl, K. Nakamura, S. S. Bulanov, S. Steinke, W. P. Leemans, Z. Kober, T. M. Ostermayr, T. Schenkel, A. J. Gonsalves, J.-L. Vay, J. van Tilborg, C. Toth, C. B. Schroeder, E. Esarey, and C. G. R. Geddes, Laser-solid interaction studies enabled by the new capabilities of the iP2 BELLA PW beamline, *Phys. Plasmas* **29**, 083102 (2022).
- [40] A. V. Kuznetsov, T. Z. Esirkepov, F. F. Kamenets, and S. V. Bulanov, Efficiency of ion acceleration by a relativistically strong laser pulse in an underdense plasma, *Plasma Phys. Rep.* **27**, 211 (2001).
- [41] S. V. Bulanov, Ion acceleration in a dipole vortex in a laser plasma corona, *Plasma Phys. Rep.* **31**, 369 (2005).
- [42] S. V. Bulanov and T. Z. Esirkepov, Comment on collimated multi-MeV ion beams from high-intensity laser interactions with underdense plasma, *Phys. Rev. Lett.* **98**, 049503 (2007).
- [43] K. Matsukado, T. Esirkepov, H. Daido, T. Utsumi, Z. Li, A. Fukumi, Y. Hayashi, S. Orimo, M. Nishiuchi, S. V. Bulanov, T. Tajima, A. Noda, Y. Iwashita, T. Shirai, T. Takeuchi, S. Nakamura, A. Yamazaki, M. Ikegami, T. Mihara, A. Morita

- et al.*, Energetic protons from a few-micron metallic foil evaporated by an intense laser pulse, *Phys. Rev. Lett.* **91**, 215001 (2003).
- [44] L. Willingale, S. P. D. Mangles, P. M. Nilson, R. J. Clarke, A. E. Dangor, M. C. Kaluza, S. Karsch, K. L. Lancaster, W. B. Mori, Z. Najmudin, J. Schreiber, A. G. R. Thomas, M. S. Wei, and K. Krushelnick, Collimated multi-MeV ion beams from high-intensity laser interactions with underdense plasma, *Phys. Rev. Lett.* **96**, 245002 (2006).
- [45] A. Yogo, H. Daido, S. V. Bulanov, K. Nemoto, Y. Oishi, T. Nayuki, T. Fujii, K. Ogura, S. Orimo, A. Sagisaka, J.-L. Ma, T. Z. Esirkepov, M. Mori, M. Nishiuchi, A. S. Pirozhkov, S. Nakamura, A. Noda, H. Nagatomo, T. Kimura, and T. Tajima, Laser ion acceleration via control of the near-critical density target, *Phys. Rev. E* **77**, 016401 (2008).
- [46] Y. Fukuda, A. Y. Faenov, M. Tampo, T. A. Pikuz, T. Nakamura, M. Kando, Y. Hayashi, A. Yogo, H. Sakaki, T. Kameshima, A. S. Pirozhkov, K. Ogura, M. Mori, T. Z. Esirkepov, J. Koga, A. S. Boldarev, V. A. Gasilov, A. I. Magunov, T. Yamauchi, R. Kodama *et al.*, Energy increase in multi-MeV ion acceleration in the interaction of a short pulse laser with a cluster-gas target, *Phys. Rev. Lett.* **103**, 165002 (2009).
- [47] L. Willingale, S. R. Nagel, A. G. R. Thomas, C. Bellei, R. J. Clarke, A. E. Dangor, R. Heathcote, M. C. Kaluza, C. Kamperidis, S. Kneip, K. Krushelnick, N. Lopes, S. P. D. Mangles, W. Nazarov, P. M. Nilson, and Z. Najmudin, Characterization of high-intensity laser propagation in the relativistic transparent regime through measurements of energetic proton beams, *Phys. Rev. Lett.* **102**, 125002 (2009).
- [48] L. Willingale, P. M. Nilson, A. G. R. Thomas, S. S. Bulanov, A. Maksimchuk, W. Nazarov, T. C. Sangster, C. Stoeckl, and K. Krushelnick, High-power, kilojoule laser interactions with near-critical density plasma, *Phys. Plasmas* **18**, 056706 (2011).
- [49] S. Göde, C. Rödel, K. Zeil, R. Mishra, M. Gauthier, F.-E. Brack, T. Kluge, M. J. MacDonald, J. Metzkes, L. Obst, M. Rehwald, C. Ruyer, H.-P. Schlenvoigt, W. Schumaker, P. Sommer, T. E. Cowan, U. Schramm, S. Glenzer, and F. Fiuzza, Relativistic electron streaming instabilities modulate proton beams accelerated in laser-plasma interactions, *Phys. Rev. Lett.* **118**, 194801 (2017).
- [50] O. Jäckel, S. M. Pfotenhauer, J. Polz, S. Steinke, H. P. Schlenvoigt, J. Heymann, A. P. L. Robinson, and M. C. Kaluza, Staged laser ion acceleration, in *Conference on Lasers and Electro-Optics/International Quantum Electronics Conference*, OSA Technical Digest (Optica Publishing Group, Washington, DC, 2009), paper JFB1.
- [51] W. P. Wang, B. F. Shen, X. M. Zhang, X. F. Wang, J. C. Xu, X. Y. Zhao, Y. H. Yu, L. Q. Yi, Y. Shi, L. G. Zhang, T. J. Xu, and Z. Z. Xu, Cascaded target normal sheath acceleration, *Phys. Plasmas* **20**, 113107 (2013).
- [52] S. Kawata, D. Sato, T. Izumiya, T. Nagashima, M. Takano, D. Barada, Y. Y. Ma, W. M. Wang, Q. Kong, P. X. Wang, and Y. J. Gu, Multi-stage ion acceleration in laser plasma interaction, *JPS Conf. Proc.* **1**, 015089 (2014).
- [53] S. M. Pfotenhauer, O. Jäckel, J. Polz, S. Steinke, H.-P. Schlenvoigt, J. Heymann, A. P. L. Robinson, and M. C. Kaluza, A cascaded laser acceleration scheme for the generation of spectrally controlled proton beams, *New J. Phys.* **12**, 103009 (2010).
- [54] X. Zhang, B. Shen, X. Li, Z. Jin, and F. Wang, Multistaged acceleration of ions by circularly polarized laser pulse: Monoenergetic ion beam generation, *Phys. Plasmas* **14**, 073101 (2007).
- [55] T. Toncian, M. Borghesi, J. Fuchs, E. d'Humieres, P. Antici, P. Audebert, E. Brambrink, C. A. Cecchetti, A. Pipahl, L. Romagnani, and O. Willi, Ultrafast laser-driven microlens to focus and energy-select mega-electron volt protons, *Science* **312**, 410 (2006).
- [56] S. Kar, H. Ahmed, R. Prasad, M. Cerchez, S. Brauckmann, B. Aurand, G. Cantono, P. Hadjisolomou, C. L. S. Lewis, A. Macchi, G. Nersisyan, A. P. L. Robinson, A. M. Schroer, M. Swantusch, M. Zepf, O. Willi, and M. Borghesi, Guided post-acceleration of laser-driven ions by a miniature modular structure, *Nat. Commun.* **7**, 10792 (2016).
- [57] S. Ferguson, P. Martin, H. Ahmed, E. Aktan, M. Alanazi, M. Cerchez, D. Doria, J. S. Green, B. Greenwood, B. Odlozilik, O. Willi, M. Borghesi, and S. Kar, Dual stage approach to laser-driven helical coil proton acceleration, *New J. Phys.* **25**, 013006 (2023).
- [58] M. Liu, S. M. Weng, H. C. Wang, M. Chen, Q. Zhao, Z. M. Sheng, M. Q. He, Y. T. Li, and J. Zhang, Efficient injection of radiation-pressure-accelerated sub-relativistic protons into laser wakefield acceleration based on 10 PW lasers, *Phys. Plasmas* **25**, 063103 (2018).
- [59] H. H. An, W. Wang, J. Xiong, C. Wang, X. Pan, X. P. Ouyang, S. Jiang, Z. Y. Xie, P. P. Wang, Y. L. Yao, N. Hua, Y. Wang, Z. C. Jiang, Q. Xiao, F. C. Ding, Y. T. Wan, X. Liu, R. R. Wang, Z. H. Fang, P. Q. Yang *et al.*, Accelerated protons with energies up to 70 MeV based on the optimized SG-II Peta-watt laser facility, *High Power Laser Sci. Eng.* **11**, e63 (2023).
- [60] V. Y. Bychenkov and G. I. Dudnikova, Two-stage laser acceleration of ions, *Plasma Phys. Rep.* **33**, 655 (2007).
- [61] A. Yogo, K. Mima, N. Iwata, S. Tosaki, A. Morace, Y. Arikawa, S. Fujioka, T. Johzaki, Y. Sentoku, H. Nishimura, A. Sagisaka, K. Matsuo, N. Kamitsukasa, S. Kojima, H. Nagatomo, M. Nakai, H. Shiraga, M. Murakami, S. Tokita, J. Kawanaka *et al.*, Boosting laser-ion acceleration with multi-picosecond pulses, *Sci. Rep.* **7**, 42451 (2017).
- [62] J. Ferri, E. Siminos, and T. Fülöp, Enhanced target normal sheath acceleration using colliding laser pulses, *Commun. Phys.* **2**, 40 (2019).
- [63] J. Kim, S. Wilks, A. Kemp, M. Sherlock, T. Ma, F. Beg, and D. Mariscal, Efficient ion acceleration by multistaged intense short laser pulses, *Phys. Rev. Res.* **4**, L032003 (2022).
- [64] H. C. Wang, S. M. Weng, M. Murakami, Z. M. Sheng, M. Chen, Q. Zhao, and J. Zhang, Cascaded acceleration of proton beams in ultrashort laser-irradiated microtubes, *Phys. Plasmas* **24**, 093117 (2017).
- [65] A. Ting, B. Hafizi, M. Helle, Y. H. Chen, D. Gordon, D. Kaganovich, M. Polyanskiy, I. Pogorelsky, M. Babzien, C. Miao, N. Dover, Z. Najmudin, and O. Ettlinger, Staging and laser acceleration of ions in underdense plasma, *AIP Conf. Proc.* **1812**, 020001 (2017).
- [66] J. B. Kim, S. Göde, and S. H. Glenzer, Development of a cryogenic hydrogen microjet for high-intensity, high-repetition rate experiments, *Rev. Sci. Instrum.* **87**, 11E328 (2016).
- [67] Z. Gong, S. S. Bulanov, T. Toncian, and A. Arefiev, Energy-chirp compensation of laser-driven ion beams enabled by structured targets, *Phys. Rev. Res.* **4**, L042031 (2022).

- [68] K. V. Lezhnin and S. V. Bulanov, Laser ion acceleration from tailored solid targets with micron-scale channels, *Phys. Rev. Res.* **4**, 033248 (2022).
- [69] X.-L. Zhu, W.-Y. Liu, M. Chen, S.-M. Weng, P. McKenna, Z.-M. Sheng, and J. Zhang, Bunched proton acceleration from a laser-irradiated cone target, *Phys. Rev. Appl.* **18**, 044051 (2022).
- [70] I. Tazes, S. Passalidis, E. Kaselouris, I. Filitis, M. Bakarezos, N. A. Papadogiannis, M. Tatarakis, and V. Dimitriou, A computational study on the optical shaping of gas targets via blast wave collisions for magnetic vortex acceleration, *High Power Laser Sci. Eng.* **10**, e31 (2022).
- [71] S. S. Bulanov, E. Esarey, C. B. Schroeder, W. P. Leemans, S. V. Bulanov, D. Margarone, G. Korn, and T. Haberer, Helium-3 and helium-4 acceleration by high power laser pulses for hadron therapy, *Phys. Rev. ST Accel. Beams* **18**, 061302 (2015).
- [72] L. Fedeli, A. Huebl, F. Boillod-Cerneux, T. Clark, K. Gott, C. Hillairet, S. Jaure, A. Leblanc, R. Lehe, A. Myers, C. Piechurski, M. Sato, N. Zaim, W. Zhang, J.-L. Vay, and H. Vincenti, Pushing the frontier in the design of laser-based electron accelerators with groundbreaking mesh-refined particle-in-cell simulations on exascale-class supercomputers, in *SC22: International Conference for High Performance Computing, Networking, Storage and Analysis* (IEEE, New York, 2022), pp. 1–12.
- [73] J.-L. Vay, A. Almgren, L. D. Amorim, I. Andriyash, D. Belkin, D. Bizzozero, A. Blelly, S. E. Clark, L. Fedeli, M. Garten, L. Ge, K. Gott, C. Harrison, A. Huebl, L. Giacomet, R. E. Groenewald, D. Grote, J. Gu, R. Jambunathan, H. Klion *et al.*, WarpX, <https://ecp-warpx.github.io>, <https://doi.org/10.5281/zenodo.4571577> (2018).
- [74] L. Obst-Huebl, K. Nakamura, S. Hakimi, J. T. D. Chant, A. Jewell, B. Stassel, A. M. Snijders, A. J. Gonsalves, J. van Tilborg, Z. Eisentraut, Z. Harvey, L. Willingale, C. Toth, C. B. Schroeder, C. G. R. Geddes, and E. Esarey, High power commissioning of BELLA iP2 up to 17 J, *Proc. SPIE* **12583**, 125805 (2023).
- [75] I. Kapchinskij and V. Vladimirskej, Limitations of proton beam current in a strong focusing linear accelerator associated with the beam space charge, in *Proceedings of the International Conference on High Energy Accelerators and Instrumentation* (CERN Scientific Information Service, Geneva, 1959), p. 274.
- [76] C. A. Lindstrøm and E. Adli, Design of general apochromatic drift-quadrupole beam lines, *Phys. Rev. Accel. Beams* **19**, 071002 (2016).
- [77] F.-E. Brack, F. Kroll, L. Gaus, C. Bernert, E. Beyreuther, T. E. Cowan, L. Karsch, S. Kraft, L. A. Kunz-Schughart, E. Lessmann, J. Metzkes-Ng, L. Obst-Huebl, J. Pawelke, M. Rehwald, H.-P. Schlenvoigt, U. Schramm, M. Sobiella, E. R. Szabó, T. Ziegler, and K. Zeil, Spectral and spatial shaping of laser-driven proton beams using a pulsed high-field magnet beamline, *Sci. Rep.* **10**, 9118 (2020).
- [78] K. D. Wang, K. Zhu, M. J. Easton, Y. J. Li, C. Lin, and X. Q. Yan, Achromatic beamline design for a laser-driven proton therapy accelerator, *Phys. Rev. Accel. Beams* **23**, 111302 (2020).
- [79] S. Busold, D. Schumacher, C. Brabetz, O. Deppert, F. Kroll, A. Blazevic, V. Bagnoud, and M. Roth, The LIGHT beamline at GSI: Shaping intense MeV proton bunches from a compact laser-driven source, in *Fifth International Particle Accelerator Conference, IPAC2014, Dresden, Germany* (JACoW Publishing, 2014), TUPME030, pp. 1419–1421.
- [80] E. D. Courant and H. S. Snyder, Theory of the alternating-gradient synchrotron, *Ann. Phys.* **3**, 1 (1958).
- [81] A. D. Piazza, L. Willingale, and J. D. Zuegel, Multi-Petawatt physics prioritization (MP3) workshop report, [arXiv:2211.13187](https://arxiv.org/abs/2211.13187).
- [82] M. Garten, S. S. Bulanov, S. Hakimi, C. E. Obst-Huebl, L. Mitchell, C. Schroeder, E. Esarey, C. G. R. Geddes, J.-L. Vay, and A. Huebl, Supplementary Materials: Laser-plasma ion beam booster based on hollow-channel magnetic vortex acceleration [Data Set], Zenodo, <https://doi.org/10.5281/zenodo.12640052>.